People's Democratic Republic Of Algeria
Ministry of Higher Education and Scientific Research

University Mohamed Boudiaf Of M'sila
Faculty Of Mathematics And Informatics
Department Of Mathematics

MASTER'S THESIS

Field: Mathematics and Informatics
Specialty : Mathematics
Option : Mathematical and Numerical Analysis

A Thesis

Legendre wavelets method for solving Volterra integral equations

By:
Achwak Nakes

Examination Committee :

Dr. *Noui* Djaidja	M.C.A,	University of M'sila	**President**.
Dr. *Amina* Khirani	M.C.A,	University of M'sila	**Supervisor**.
Dr. *Nabila* Seghiri	M.C.B,	University of M'sila	**Examiner**.

Academic Year
2025/2026

◊ الإهداء ◊

﴿وَآخِرُ دَعْوَاهُمْ أَنِ الْحَمْدُ لِلَّهِ رَبِّ الْعَالَمِينَ﴾

[سورة يونس: الآية 10]

لم تكن الرحلة قصيرةً ولا سهلةً، ولم يكن الطريق محفوفاً بالتسهيلات، ولكنني بفضل الله تجاوزتُ الصعاب. ها أنا ذا أصل إلى نهاية رحلتي الجامعية بعد كفاحٍ ومشقة استمرّا خمس سنوات في سبيل العلم وتحقيق الحلم؛ سنوات حملت في طياتها الكثير من التحديات والأمنيات، ليصبح سعيُ الأمس واقعاً أعيشه اليوم.

الحمد لله الذي يسّر لنا البدايات، وأعاننا حتى بلغنا النهايات بفضله وكرمه.

أهدي هذا العمل المتواضع لنفسي أولاً؛ تقديراً لثباتها، ثم إلى كل من ساندني ووقف بجانبي لإتمام هذه المسيرة، فكانوا لي سنداً قريباً لا يلين ولا ينقطع.

إلى من أوصلاني إلى ما أنا عليه الآن، وسهرا الليالي من أجل راحتي، من أمرني الله ببرّهما والإحسان إليهما:

``وَاخْفِضْ لَهُمَا جَنَاحَ الذُّلِّ مِنَ الرَّحْمَةِ وَقُل رَّبِّ ارْحَمْهُمَا كَمَا رَبَّيَانِي صَغِيرًا"

إلى من جعل الله الجنة تحت قدميها، ونبع الحنان الذي يغمرني، من كانت دعواتها تحرسني وتسعد قلبي في كل حين، قرّة عيني وسرّ نجاحي وملجئي.. **أمي الغالية.**

إلى من كدّ وتعب وتورّم جبينه عرقاً لأجلي، من علمني أن النجاح لا يُنال إلا بالصبر والعزيمة، النور الذي يضيء طريقي.. **والدي العزيز.**

إلى سندي الثابت وأمان أيامي، إخوتي وأخواتي الذين شددتُ بهم عضدي، فكانوا لي نبعاً أرتوي منه صفاء الحياة ومحبتها.

إلى من كانت لي أختاً قبل أن تكون صديقة رحابي وفاء شكراً لكِ على صدقكِ ودعمكِ ومرافقتكِ لي في هذا المشوار العلمي فلكِ جزء من هذَا النجاح

إلى صديقات قلبي الوفيات، اللاتي سكنَّ الوتين، كُنْتُنَّ أجمل النعم التي أدعو الله دائماً دوامها.

إلى كل من أسعدني، ولو بكلمة طيبة أو دعوة صادقة، طوال مسيرتي في إعداد هذه المذكرة.

إلى كل من عقد العزم على بلوغ هدفه فناله، فالحمد لله الذي بنعمته تتم الصالحات، والحمد لله شكراً وحباً وامتناناً في البدء وفي الختام.

Notations

$\mathbb{N}$	The set of natural numbers.
$L^2(\mathbb{R})$	Square-integrable functions space.
$\psi(x)$	Mother wavelet.
$\psi_{nm}(x)$	Legendre wavelets.
$p_m(x)$	Legendre polynomial.
k	Dilation parameter.
n	Translation parameter.
m	Order of Legendre polynomial.
M	Maximum polynomial order.
$\{u_n(x)\}, \{g_n(t)\}$	Successive approximations sequence.
$\varphi_n(t)$	Difference function.
c_{nm}	Expansion coefficients.
$\phi_n(t)$	Temporal baseline function.
F, K	Upper bounds constants.
T	Domain upper bound.

List of Tables

List of Figures

Contents

Introduction

Integral equations have emerged as a vital mathematical framework for modeling a myriad of phenomena across physics, engineering, and biological sciences. Among these, Volterra integral equations (VIEs) play a pivotal role in describing evolutionary processes with memory effects, such as viscoelastic materials, population dynamics, and heat conduction in materials with fading memory. Due to the inherent complexity of analytical methods, obtaining exact solutions for many practical forms of VIEs is often intensive or analytically intractable. Consequently, the development of stable, fast, and high-precision numerical techniques has become a primary focus in modern numerical analysis.

In recent decades, wavelet-based numerical techniques have gained substantial attention due to their exceptional capability to resolve localized variations, singularities, and sharp gradients in functions. Wavelets provide a multi-resolution analysis framework that transforms continuous calculus problems into localized linear systems. Among various orthogonal family bases, Legendre wavelets stand out as a highly efficient choice. Constructed by combining the localization properties of compact support wavelets with the global smoothing features of Legendre polynomials, they offer significant computational advantages. Specifically, they possess vanishing moments, strict orthogonality, and explicit operational matrices of integration, which dramatically lower numerical overhead and bound error propagation.

The primary objective of this Master's thesis is to systematically implement and evaluate the Legendre Wavelet Method (LWM) paired with the collocation technique for solving linear second-kind Volterra integral equations. By exploiting the operational matrix of integration, the continuous integral operator is effectively mapped into an algebraic system of linear equations, which can be readily inverted to obtain continuous approximations. Furthermore, a rigorous mathematical framework is presented to guarantee the existence, uniqueness, and structural error convergence rates of the scheme.

To provide a clear and comprehensive exposition of this study, the thesis is structured into

three foundational chapters:

- **Chapter 1 (Preliminaries):** Establishes the core functional analysis backdrop, including Banach spaces, discrete wavelet properties, and the mathematical derivation of the Legendre wavelets operational matrix of integration alongside the collocation technique setup.
- **Chapter 2 (Integral Equations):** Outlines the mathematical classification of integral operators, details the Picard iteration scheme, and presents rigorous proofs for the existence and uniqueness of solutions to linear second-kind Volterra integral equations.
- **Chapter 3 (Numerical Solutions and Convergence Analysis):** Focuses on the global matrix representation, provides detailed applications on various benchmark numerical examples, and delivers a comparative analysis highlighting the rapid convergence rate achieved by increasing the polynomial order.

CHAPTER 1

PRELIMINARIES

The chapter established the foundational mathematical framework required for the subsequent analysis. We begin by introducing essential concepts from functional analysis, specifically the definitions of **seminorms, normed spaces, and Banach spaces**. These core principles provide the theoretical basis for the construction and application of **Legendre wavelets**. Following this, we detail the properties of Legendre polynomials, the function approximation method, and the derivation of the operational matrix of integration, which serves as a vital tool for solving the integral equations addressed in this work.

1.1 Basic Definitions

Definition 1.1. Let V be a vector space (over the real or complex numbers). A function, $\|\cdot\|$, from V into the non-negative real numbers is called a **seminorm** on V if it satisfies the following two properties:

a) $\|v+w\| \leq \|v\| + \|w\|$ for all $v, w \in V$.

b) $\|sv\| = |s|\|v\|$ for all $v \in V$ and all scalars s.

Definition 1.2. A seminorm, $\|\cdot\|$, is called a **norm** if, in addition, it satisfies the following property:

c) If $v \in V$ and $\|v\| = 0$, then $v = 0$.

Definition 1.3. A **normed vector space** (or, more briefly, a **normed space**) is a vector space V together with a particular norm on V.

Definition 1.4. A **Banach space** is a normed space which is complete (with respect to the metric obtained from its norm).

In other words, a Banach space is a normed space which has the property that every Cauchy sequence of elements of the space has a limit. That is,

$$\{f_n\}_{n\in\mathbf{N}} \text{ is Cauchy in } X \quad \Longrightarrow \quad \exists f \in X \text{ such that } f_n \to f.$$

Definition 1.5. Convergence Let X be a normed linear space (such as an inner product space), and let $\{f_n\}_{n\in\mathbf{N}}$ be a sequence of elements of X.

(a) We say that $\{f_n\}_{n\in\mathbf{N}}$ *converges* to $f \in X$, and write $f_n \to f$, if

$$\lim_{n\to\infty} \|f - f_n\| = 0,$$

i.e.,

$$\forall \varepsilon > 0,\ \exists N > 0 \text{ such that } n > N \Longrightarrow \|f - f_n\| < \varepsilon.$$

(b) We say that $\{f_n\}_{n\in\mathbf{N}}$ is *Cauchy* if

$$\forall \varepsilon > 0,\ \exists N > 0 \text{ such that } m, n > N \Longrightarrow \|f_m - f_n\| < \varepsilon.$$

Definition 1.6. Convergent Series Let $\{f_n\}_{n\in\mathbf{N}}$ be a sequence of elements of a normed linear space X. Then the series $\sum_{n=1}^{\infty} f_n$ *converges* and *equals* $f \in X$ if the *partial sums* $s_N = \sum_{n=1}^{N} f_n$ converge to f, i.e., if

$$\|f - s_N\| = \left\| f - \sum_{n=1}^{N} f_n \right\| \to 0 \quad \text{as } N \to \infty.$$

Definition 1.7. Absolutely Convergent Series Let X be a normed space and let $\{f_n\}_{n\in\mathbf{N}}$ be a sequence of elements of X. If

$$\sum_{n=1}^{\infty} \|f_n\| < \infty,$$

then we say that the series $\sum_n f_n$ is *absolutely convergent* in X.

Note that the definition of absolute convergence does not by itself tell us that the series $\sum_n f_n$ actually converges. That is always true if X is a Banach space, but need not be true if X is not complete.

1.2 Legendre Wavelets

Wavelets comprise a class of functions formed by translation and dilation of a single function called mother wavelet $\psi(x)$ that is given as:

$$\psi_{a,b}(x) = \frac{1}{\sqrt{|a|}}\psi\left(\frac{x-b}{a}\right), \quad a, b \in \mathbb{R}, \quad a \neq 0$$

where a and b are the dilation and translation parameters, respectively. Limiting a and b to discrete values as $a = a_0^{-j}$ and $b = kb_0a_0^{-j}$, where $a_0 > 1, b_0 > 1$ and $j, k \in \mathbb{N}$, we can find a class of discrete wavelets as follows:

$$\psi_{j,k}(x) = |a_0|^{\frac{j}{2}}\,\psi\left(a_0^j x - kb_0\right).$$

This set of wavelets forms an orthogonal base for $L^2(\mathbb{R})$.

1.3 Legendre polynomial

The Legendre polynomial of order m represented by $p_m(x)$ is defined on the interval $[-1, 1]$ by the following recurrence formula:

$$p_0(x) = 1$$
$$p_1(x) = x$$
$$p_{m+2}(x) = \frac{2m+3}{m+2}xp_{m+1}(x) - \frac{m+1}{m+2}p_m(x) \quad m = 0, 1, 2, \ldots$$

The $m = 0$ Legendre polynomial is: 1

The $m = 1$ Legendre polynomial is: x

The $m = 2$ Legendre polynomial is: $\frac{1}{2}(-1 + 3x^2)$

The $m = 3$ Legendre polynomial is: $\frac{1}{2}(-3x + 5x^3)$

The $m = 4$ Legendre polynomial is: $\frac{1}{8}(3 - 30x^2 + 35x^4)$

The $m = 5$ Legendre polynomial is: $\frac{1}{8}(15x - 70x^3 + 63x^5)$

The $m = 6$ Legendre polynomial is: $\frac{1}{16}(-5 + 105x^2 - 315x^4 + 231x^6)$

The $m = 7$ Legendre polynomial is: $\frac{1}{16}(-35x + 315x^3 - 693x^5 + 429x^7)$

Lemma 1.1. *(Orthogonality of Legendre polynomials). Legendre polynomials $P_n(x)$ of distinct degrees are orthogonal over $[-1, 1]$, with weighting function $w(x) = 1$.*

Proof. It is well-established in linear algebra that the orthogonality of two continuous functions $f_m(x)$ and $f_n(x)$ over a domain $[a, b]$ is equivalent to the nullity of the inner product $\langle f_m|f_n\rangle := \int_a^b f_m(x)f_n(x)w(x)\,dx$. On taking $w(x) = 1$, all we have to do is to show that

$$\int_{-1}^{+1} P_m(x) \cdot P_n(x)\,dx = 0, \quad \forall m \neq n. \tag{1.1}$$

Since all $P_n(x)$ satisfy Legendre's ODE, we have

$$\left[(1-x^2)P_n'(x)\right]' + n(n+1)P_n = 0 \tag{1.2}$$

and

$$\left[(1-x^2)P_m'(x)\right]' + m(m+1)P_m = 0. \tag{1.3}$$

Now, multiply both sides of Eq. (1.2) by $P_m(x)$ and those of Eq. (1.3) by $P_n(x)$. A member-to-member subtraction of the resulting expressions will result in

$$\left[(1-x^2)(P_m'P_n - P_mP_n')\right]' + (m-n)(m+n+1)P_mP_n = 0. \tag{1.4}$$

Finally, the integration of both sides over the domain $[-1, 1]$ will yield

$$\int_{-1}^{+1} \frac{d}{dx}\left[(1-x^2)(P_m'P_n - P_mP_n')\right]\,dx + (m-n)(m+n+1)\int_{-1}^{+1} P_mP_n\,dx = 0. \tag{1.5}$$

From the fundamental theorem of calculus, the first integral is always null, so

$$(m-n)(m+n+1)\int_{-1}^{+1} P_mP_n\,dx = 0. \tag{1.6}$$

Clearly, for all non-negative values of $m \neq n$ the last integral has to be null.

Graphical Analysis of Legendre Polynomials

To provide a clearer understanding of the analytical forms previously defined, Figure 1.1 illustrates the first eight Legendre polynomials $P_n(x)$ over the interval $[-1, 1]$. As observed in the plot, the polynomials satisfy the boundary conditions $P_n(1) = 1$ and $P_n(-1) = (-1)^n$, and they exhibit an increasing number of roots as the degree n increases, which is consistent with the properties of orthogonal basis functions.

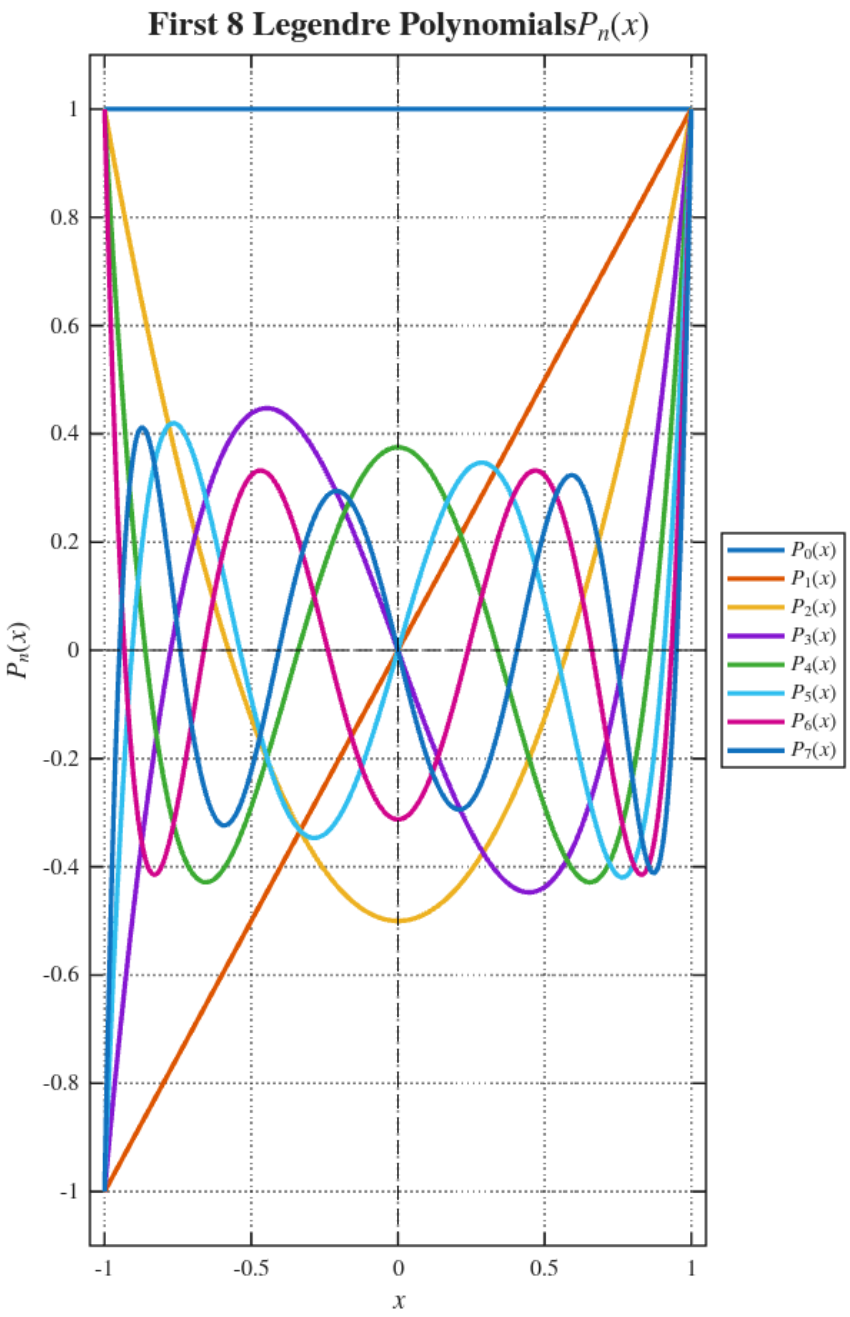

Figure 1.1: The first eight Legendre polynomials $P_n(x)$ for $n = 0, 1, \ldots, 7$ on the domain $[-1, 1]$.

The Legendre wavelets are given over the range $[0, 1)$ as:

$$\psi_{nm}(x) = \begin{cases} \left(m + \frac{1}{2}\right)^{\frac{1}{2}} 2^{\frac{k}{2}} p_m\left(2^k x - 2n + 1\right), & \frac{n-1}{2^{k-1}} \leq x < \frac{n}{2^{k-1}} \\ 0, & \text{otherwise} \end{cases} \tag{1.7}$$

where $k \in \mathbb{N}, n = 1, 2, 3, \ldots, 2^{k-1}$ and $m = 0, 1, 2, \ldots, M-1; m$ denotes the order of the Legendre polynomial, and M is a positive integer.

1.4 Visual Representation of Legendre Wavelets

The behavior of Legendre wavelets can be better understood through their visual representations. Figure 1.2 illustrates the first eight basis functions of the Legendre wavelets. These plots demonstrate the increasing oscillation and complexity of the functions as the order m increases, which is a characteristic property of orthogonal polynomials used in function approximation.

1.5 Function Approximation

A function $f(t)$ defined over $[0, 1)$ may be expanded as

$$f(t) = \sum_{n=1}^{\infty} \sum_{m=0}^{\infty} c_{nm} \psi_{nm}(t), \tag{1.8}$$

where the coefficients $c_{n,m}$ are determined by the inner product

$$c_{n,m} = \big(f(t), \psi_{nm}(t)\big). \tag{1.9}$$

If the infinite series in Equation (1.8) is truncated, it can be written as

$$f(t) \cong \sum_{n=1}^{2^{k-1}} \sum_{m=0}^{M-1} c_{nm} \psi_{nm}(t) = C^{\mathrm{T}} \Psi(t), \tag{1.10}$$

where C and $\Psi(t)$ are $2^{k-1}M \times 1$ vectors given by

$$C = \left[c_{10}, c_{11}, \ldots, c_{1,M-1}, c_{20}, \ldots, c_{2,M-1}, \ldots, c_{2^{k-1},0}, \ldots, c_{2^{k-1},M-1}\right]^{\mathrm{T}}, \tag{1.11}$$

$$\Psi(t) = \left[\psi_{10}(t), \psi_{11}(t), \ldots, \psi_{1,M-1}(t), \psi_{20}(t), \ldots, \psi_{2,M-1}(t), \ldots, \psi_{2^{k-1},0}(t), \ldots, \psi_{2^{k-1},M-1}(t)\right]^{\mathrm{T}}. \tag{1.12}$$

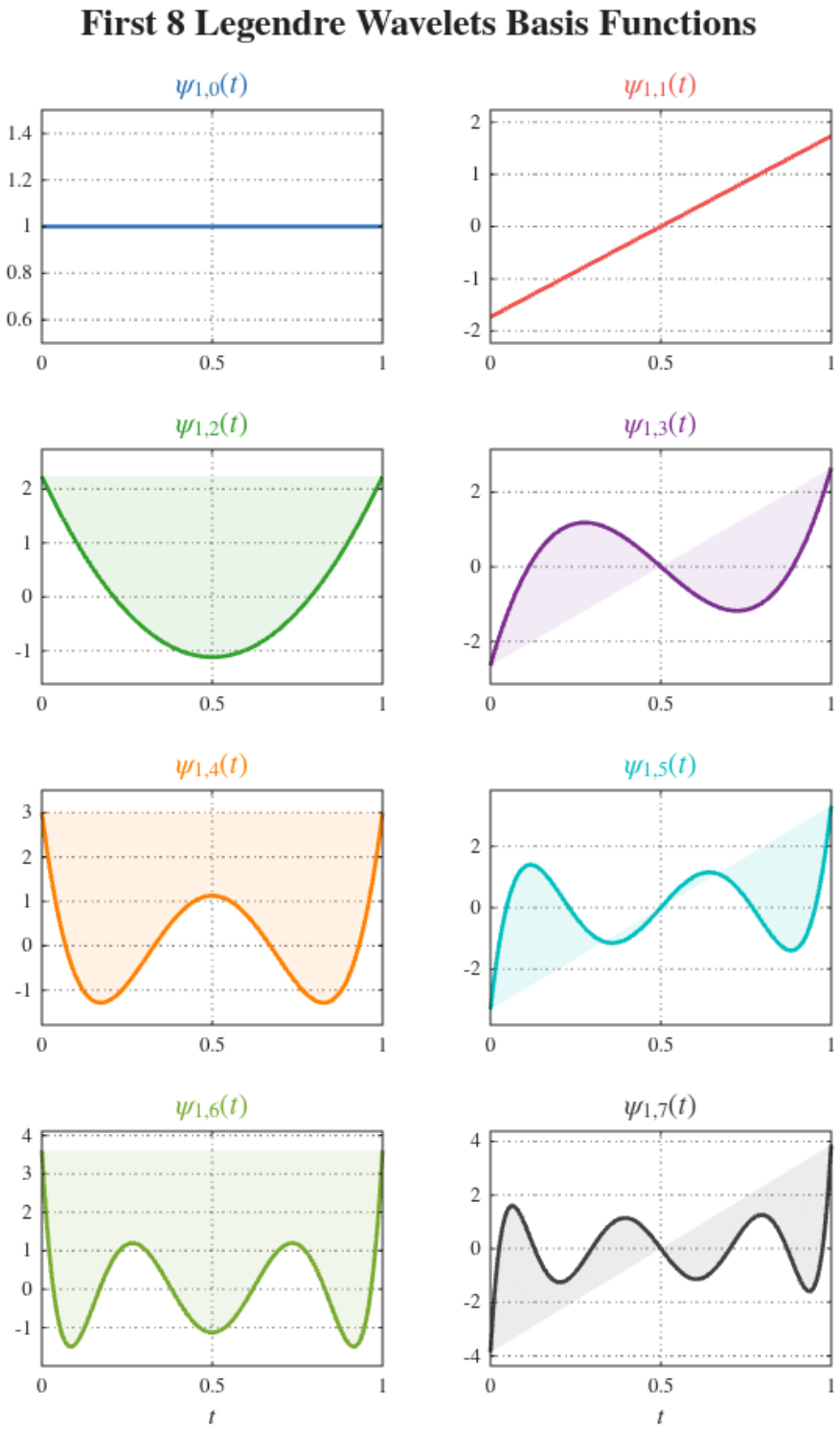

Figure 1.2: The first eight Legendre wavelets basis functions, illustrating the varying degrees of the polynomials over the interval $[0, 1]$.

1.6 Legendre wavelets operational matrix of integration

In this section the operational matrix of integration P will be derived. First, we find the matrix P with $M = 3$ and $k = 2$. The six basis functions are given by

$$\left.\begin{aligned} \psi_{10} &= 2^{1/2}, \\ \psi_{11} &= 6^{1/2}(4t-1), \\ \psi_{12} &= (10)^{1/2}\left[\frac{3}{2}(4t-1)^2 - \frac{1}{2}\right], \end{aligned}\right\} \quad 0 \le t < \frac{1}{2}, \tag{1.13}$$

and

$$\left.\begin{aligned} \psi_{20} &= 2^{1/2}, \\ \psi_{21} &= 6^{1/2}(4t-3), \\ \psi_{22} &= (10)^{1/2}\left[\frac{3}{2}(4t-3)^2 - \frac{1}{2}\right], \end{aligned}\right\} \quad \frac{1}{2} \le t < 1. \tag{1.14}$$

By integrating Equations (1.13) and (1.14) from 0 to t , we obtain

$$\begin{aligned} \int_0^t \psi_{10}(t)\,dt &= \begin{cases} 2^{1/2}t & 0 \le t < \frac{1}{2} \\ \frac{2^{1/2}}{2}, & \frac{1}{2} \le t < 1, \end{cases} \\ &= \frac{1}{4}\psi_{10}(t) + \frac{2^{1/2}}{4\times 6^{1/2}}\psi_{11} + \frac{1}{2}\psi_{20} \\ &= \left[\frac{1}{4}, \frac{2^{1/2}}{4\times 6^{1/2}}, 0, \frac{1}{2}, 0, 0\right]^T \Psi_6(t). \end{aligned}$$

Thus

$$\int_0^t \Psi_{6\times 1}(t)\,dt = P_{6\times 6}\Psi_6(t), \tag{1.15}$$

Where

$$\Psi_6(t) = [\psi_{10}, \psi_{11}, \psi_{12}, \psi_{20}, \psi_{21}, \psi_{22}]^T \tag{1.16}$$

where the matrix $P_{6\times 6}$ is:

$$P_{6\times 6} = \frac{1}{4}\begin{bmatrix} 1 & \frac{2^{1/2}}{6^{1/2}} & 0 & 2 & 0 & 0 \\ -\frac{3^{1/2}}{3} & 0 & \frac{3^{1/2}}{3\times 5^{1/2}} & 0 & 0 & 0 \\ 0 & -\frac{5^{1/2}}{5\times 3^{1/2}} & 0 & 0 & 0 & 0 \\ 0 & 0 & 0 & 1 & \frac{2^{1/2}}{6^{1/2}} & 0 \\ 0 & 0 & 0 & -\frac{3^{1/2}}{3} & 0 & \frac{3^{1/2}}{3\times 5^{1/2}} \\ 0 & 0 & 0 & 0 & -\frac{5^{1/2}}{5\times 3^{1/2}} & 0 \end{bmatrix} \tag{1.17}$$

The matrix $P_{6\times 6}$ can be partitioned as:

$$P_{6\times 6} = \begin{bmatrix} L_{3\times 3} & F_{3\times 3} \\ 0_{3\times 3} & L_{3\times 3} \end{bmatrix}$$

where:

$$L_{3\times3} = \frac{1}{4}\begin{bmatrix} 1 & \frac{2^{1/2}}{6^{1/2}} & 0 \\ -\frac{3^{1/2}}{3} & 0 & \frac{3^{1/2}}{3\times5^{1/2}} \\ 0 & -\frac{5^{1/2}}{5\times3^{1/2}} & 0 \end{bmatrix}, \quad F_{3\times3} = \frac{1}{4}\begin{bmatrix} 2 & 0 & 0 \\ 0 & 0 & 0 \\ 0 & 0 & 0 \end{bmatrix}$$

In general, we have

$$\int_0^t \Psi(\tau)\, d\tau = P\Psi(t)$$

where $\Psi(t)$ is given in (1.7) and P is a $(2^{k-1}M) \times (2^{k-1}M)$ matrix given by

$$P = \frac{1}{2^k}\begin{bmatrix} L & F & F & \dots & F \\ 0 & L & F & \dots & F \\ \vdots & 0 & \ddots & \ddots & \vdots \\ \vdots & \vdots & \ddots & \ddots & F \\ 0 & 0 & \dots & 0 & L \end{bmatrix},$$

where F and L are $M \times M$ matrices given by

$$F = \begin{bmatrix} 2 & 0 & \dots & 0 \\ 0 & 0 & \dots & 0 \\ \vdots & \vdots & \vdots & \vdots \\ 0 & 0 & \dots & 0 \end{bmatrix},$$

and

$$L = \begin{bmatrix} 1 & \frac{1}{3^{1/2}} & 0 & 0 & \dots & 0 & 0 & 0 \\ -\frac{3^{1/2}}{3} & 0 & \frac{3^{1/2}}{3\times5^{1/2}} & 0 & \dots & 0 & 0 & 0 \\ 0 & -\frac{5^{1/2}}{5\times3^{1/2}} & 0 & \frac{5^{1/2}}{5\times7^{1/2}} & \ddots & 0 & 0 & 0 \\ 0 & 0 & -\frac{7^{1/2}}{7\times5^{1/2}} & 0 & \ddots & 0 & 0 & 0 \\ \vdots & \vdots & \vdots & \vdots & \ddots & \ddots & \ddots & \vdots \\ 0 & 0 & 0 & 0 & \dots & -\frac{(2M-3)^{1/2}}{(2M-3)(2M-5)^{1/2}} & 0 & \frac{(2M-3)^{1/2}}{(2M-3)(2M-1)^{1/2}} \\ 0 & 0 & 0 & 0 & \dots & 0 & -\frac{(2M-1)^{1/2}}{(2M-1)(2M-3)^{1/2}} & 0 \end{bmatrix}.$$

The operational matrix technique utilized herein was originally derived based on the framework established by [13].

1.7 The Collocation Method

The collocation method is a highly efficient and widely utilized numerical technique in numerical analysis. Its primary advantage lies in its ability to transform a continuous problem into an easily computable system of algebraic equations. In this study, the approximate solution is forced to satisfy the original equation precisely at a set of discretely selected points known as collocation points.

To maintain perfect compatibility with the discrete wavelet basis representation, **equidistantly spaced nodes (uniform nodes)** are selected within the interval $[0, 1]$. The total number of collocation points, denoted by N, is intrinsically determined by the dilation parameter k and the degree of Legendre polynomial M according to the relation:

$$N = 2^{k-1} \times M \tag{1.18}$$

Configured by this framework, the discrete collocation nodes x_i are generated mathematically across the domain as follows:

$$x_i = \frac{i-1}{N-1}, \quad i = 1, 2, \ldots, N \tag{1.19}$$

This structured grid choice ensures that the collocation nodes strictly align with the operational setup, allowing for an accurate and stable formulation of the matrices.

CHAPTER 2

INTEGRAL EQUATIONS

In this chapter, we will outline the classifications of integral equations and establish the existence and uniqueness of the solution for the Volterra integral equation.

2.1 The classifications of integral equations

An integral equation is an equation in which the unknown function $u(x)$ appears under an integral . A standard integral equation in $u(x)$ is of the form:

$$u(x) = f(x) + \lambda \int_{g(x)}^{h(x)} K(x,t)u(t)\,dt, \tag{2.1}$$

where $g(x)$ and $h(x)$ are the limits of integration, λ is a constant parameter, and $K(x,t)$ is a function of two variables x and t called the *kernel* or the *nucleus* of the integral equation.

Integral equations appear in many types. The types depend mainly on the limits of integration and the kernel of the equation. In this text we will be concerned with the following types of integral equations.

Fredholm Integral Equations

For Fredholm integral equations, the limits of integration are fixed. Moreover, the unknown function $u(x)$ may appear only inside integral equation in the form:

$$f(x) = \int_a^b K(x,t)u(t)\,dt. \tag{2.2}$$

This is called Fredholm integral equation of the *first kind*. However, for like

$$\int_0^1 (x+t)u(t)\,dt = f(x) \tag{2.3}$$

Fredholm integral equations of the *second kind*, the unknown function $u(x)$ appears inside and outside the integral sign. The second kind is represented by the form:

$$u(x) = f(x) + \lambda \int_a^b K(x,t)u(t)\,dt. \tag{2.4}$$

for example

$$u(x) = 1 + \int_0^1 xt\, u(t)\, dt \tag{2.5}$$

Volterra Integral Equations

In Volterra integral equations, at least one of the limits of integration is a variable. For the *first kind* Volterra integral equations, the unknown function $u(x)$ appears only inside integral sign in the form:

$$f(x) = \int_0^x K(x,t)u(t)\, dt. \tag{2.6}$$

for example

$$\int_0^x e^{x-t}u(t)\, dt = \sin(x) \tag{2.7}$$

However, Volterra integral equations of the *second kind*, the unknown function $u(x)$ appears inside and outside the integral sign. The second kind is represented by the form:

$$u(x) = f(x) + \lambda \int_0^x K(x,t)u(t)\, dt. \tag{2.8}$$

for example

$$u(x) = x^2 + \int_0^x (x-t)u(t)\, dt \tag{2.9}$$

If we set $f(x) = 0$ in Fredholm or Volterra integral equation of the second kind given by (2.4) and (2.8), the resulting equation is called a *homogeneous* integral equation, otherwise it is called *nonhomogeneous* integral equation.

2.2 Existence and Uniqueness of the Solution of Second-Kind Linear Volterra Integral Equations.

The classical approach to proving the existence and uniqueness of the solution of (2.8) is the method of successive approximation, also called the Picard method. This consists of the simple iteration

$$g_n(t) = f(t) + \int_0^t k(t,s)g_{n-1}(s)ds, \quad n = 1, 2, \ldots \tag{2.10}$$

with

$$g_0(t) = f(t).$$

For ease of manipulation it is convenient to introduce

$$\varphi_n(t) = g_n(t) - g_{n-1}(t), \quad n = 1, 2, \ldots \tag{2.11}$$

with

$$\varphi_0(t) = f(t).$$

On subtracting from (2.10) the same equation with n replaced by $n-1$, we see that

$$\varphi_n(t) = \int_0^t k(t,s)\varphi_{n-1}(s)ds, \quad n = 1, 2, \ldots \tag{2.12}$$

Also (2.11)

$$g_n(t) = \sum_{i=0}^{n} \varphi_i(t). \tag{2.13}$$

The first theorem uses this iteration to prove the existence and uniqueness of the solution under quite restrictive conditions, namely that $k(t,s)$ and $f(t)$ are continuous.

Theorem 2.1. *If $k(t,s)$ is continuous in $0 \leqslant s \leqslant t \leqslant T$ and $f(t)$ is continuous in $0 \leqslant t \leqslant T$, then the integral equation* (2.8)*possesses a unique continuous solution for $0 \leqslant t \leqslant T$.*

Proof. Choose F and K such that

$$\begin{aligned} |f(t)| &\leqslant F, \qquad 0 \leqslant t \leqslant T, \\ |k(t,s)| &\leqslant K, \quad 0 \leqslant s \leqslant t \leqslant T. \end{aligned}$$

We first prove by induction that

$$|\varphi_n(t)| \leqslant \frac{F(Kt)^n}{n!}, \quad 0 \leqslant t \leqslant T, \quad n = 0, 1, \ldots \tag{2.14}$$

If we assume that (2.14) is true for $n-1$, then from (2.12)

$$|\varphi_n(t)| \leqslant \frac{FK^n}{(n-1)!}\int_0^t s^{n-1}ds = \frac{FK^n t^n}{n!}.$$

Since (2.14) is obviously true for $n = 0$, it holds for all n. This bound makes it obvious that the sequence $g_n(t)$ in (2.13) converges and we can write

$$g(t) = \sum_{i=0}^{\infty} \varphi_i(t). \tag{2.15}$$

We now show that this $g(t)$ satisfies equation (2.8) The series (2.15)is uniformly convergent since the terms $\varphi_i(t)$ are dominated by $F(KT)^i/i!$. Hence we can interchange the order of integration and summation in the following expression to obtain

$$\begin{aligned} \int_0^t k(t,s)\sum_{i=0}^{\infty}\varphi_i(s)ds &= \sum_{i=0}^{\infty}\int_0^t k(t,s)\varphi_i(s)ds \\ &= \sum_{i=0}^{\infty}\varphi_{i+1}(t) = \sum_{i=0}^{\infty}\varphi_i(t) - f(t) \end{aligned}$$

This proves that $g(t)$ defined by (2.15)satisfies equation (2.8). Each of the $\varphi_i(t)$ is clearly continuous. Therefore $g(t)$ is continuous, since it is the limit of a uniformly convergent sequence of continuous functions. To show that $g(t)$ is the only continuous solution, suppose there exists another continuous solution $\tilde{g}(t)$ of (2.8). Then

$$g(t) - \tilde{g}(t) = \int_0^t k(t,s)g(s) - \tilde{g}(s)ds \tag{2.16}$$

Since $g(t)$ and $\tilde{g}(t)$ are both continuous, there exists a constant B such that

$$|g(t) - \tilde{g}(t)| \leqslant B, \quad 0 \leqslant t \leqslant T.$$

Substituting this into (2.16)

$$|g(t) - \tilde{g}(t)| \leqslant KBt, \quad 0 \leqslant t \leqslant T,$$

and repeating the step shows that

$$|g(t) - \tilde{g}(t)| \leqslant \frac{B(Kt)^n}{n!}, \quad 0 \leqslant t \leqslant T,$$

for any n. For large enough n, the right-hand side is arbitrarily small, so that we must have

$$g(t) = \tilde{g}(t), \quad 0 \leqslant t \leqslant T,$$

and there is only one continuous solution. Note that although there is only one continuous solution, there may be solutions which are not continuous. One well-known example is the equation

$$g(t) = \int_0^t s^{t-s} g(s)ds, \tag{2.17}$$

which has one obvious solution $g(t) = 0$. The kernel s^{t-s} is continuous, but it can be verified that

$$g(t) = ct^{t-1} \tag{2.18}$$

is a solution of (2.17) for any c. For $c \neq 0$ this solution is discontinuous at $t = 0$. It is not difficult to show that any discontinuous solution of (2.8)must be nonintegrable and this is true of (2.18) □

The detailed proof can be found here [12].

2.3 Method of Successive Approximations (Picard Iteration)

The method of successive approximations provides a systematic iterative scheme to solve the linear Volterra integral equation of the second kind. The core principle lies in generating a sequence of functions $\{u_n(x)\}_{n=0}^{\infty}$ that converges to the exact solution $u(x)$. The process is initiated by selecting an initial guess $u_0(x)$, typically $u_0(x) = f(x)$ or $u_0(x) = 0$. The subsequent approximations are then obtained through the recurrence relation:

$$u_n(x) = f(x) + \lambda \int_0^x K(x,t)u_{n-1}(t)dt, \quad n = 1, 2, 3, \ldots$$

As n increases, the error between the approximation $u_n(x)$ and the actual solution $u(x)$ vanishes, provided the continuity conditions for $f(x)$ and $K(x,t)$ are satisfied.

Illustrative Example

To illustrate the practical application of the Picard method, consider the following Volterra integral equation:

$$u(x) = 1 + \int_0^x u(t)dt$$

We begin the iteration with the simplest initial guess, $u_0(x) = 1$.

(u_1): Substituting $u_0(t) = 1$ into the integral:

$$u_1(x) = 1 + \int_0^x (1)dt = 1 + [t]_0^x = 1 + x$$

(u_2): Substituting the previously found $u_1(t) = 1 + t$:

$$u_2(x) = 1 + \int_0^x (1+t)dt = 1 + [t + \frac{t^2}{2}]_0^x = 1 + x + \frac{x^2}{2}$$

(u_3): Continuing the process with $u_2(t)$:

$$u_3(x) = 1 + \int_0^x (1 + t + \frac{t^2}{2})dt = 1 + x + \frac{x^2}{2!} + \frac{x^3}{3!}$$

By observing the pattern in the sequence $u_n(x) = \sum_{k=0}^{n} \frac{x^k}{k!}$, it becomes evident that as $n \to \infty$, the sequence converges to the Taylor series of the exponential function. Thus, the exact solution is:

$$u(x) = e^x$$

CHAPTER 3

NUMERICAL SOLUTIONS FOR LINEAR VOLTERRA INTEGRAL EQUATIONS USING LEGENDRE WAVELETS METHOD

In this chapter, we present the implementation of the Legendre wavelets method to compute numerical solutions for linear Volterra integral equations of the second kind. The core mathematical principle relies on converting the continuous integral equation into an algebraic system of linear equations via discretization at specific collocation nodes, which can then be solved directly using matrix inversion.

3.1 Matrix Representation and Discretization Method

Consider the nonhomogeneous linear Volterra integral equation of the second kind defined by

$$y(x) = f(x) + \int_0^x K(x,t)y(t)\,dt; x \in [0,1)$$

where:

$f(x)$ represents the right-hand input function, $K(x,t)$ is the continuous integral kernel, and $y(x)$ is the unknown target solution function to be approximated.

By truncating the infinite series expansion of the Legendre wavelets, the unknown function $y(x)$ is represented by its finite projection onto the wavelet basis subspace:

$$y(x) \approx \sum_{n=1}^{2^{k-1}} \sum_{m=0}^{M-1} c_{n,m}\psi_{n,m}(x) = C^T\Psi(x)$$

where C and $\Psi(x)$ are $N \times 1$ vectors with dimension:

$$N = 2^{k-1}M$$

The expanded expansion coefficient vector C and the basis vector $\Psi(x)$ are defined respectively as:

$$C = [c_{1,0}, c_{1,1}, \ldots, c_{1,M-1}, c_{2,0}, \ldots, c_{2^{k-1},M-1}]^T$$

$$\Psi(x) = [\psi_{1,0}(x), \psi_{1,1}(x), \ldots, \psi_{1,M-1}(x), \psi_{2,0}(x), \ldots, \psi_{2^{k-1},M-1}]^T$$

To determine the unknown coefficient vector C, we apply the collocation method by choosing N equidistant collocation nodes x_i distributed within the range $[0, 1)$:

$$x_i = \frac{i-1}{N-1}, \quad i = 1, 2, \ldots, N$$

Evaluating the vector equation at these exact collocation spatial coordinates transforms the integral formulation into:

$$C^T\Psi(x_i) = f(x_i) + \int_0^{x_i} K(x_i, t)C^T\Psi(t)\, dt$$

In global matrix notation, this discrete algebraic structure translates into a system of linear expressions represented by:

$$(\Psi - W)C = F$$

where the load vector is:

$$F = [f(x_1), f(x_2), \ldots, f(x_N)]^T$$

Ψ is the $N \times N$ wavelet basis evaluation matrix:

$$\Psi_{i,j} = \psi_j(x_i)$$

and W is the $N \times N$ localized Volterra integration operational matrix whose individual entries are evaluated via the definite integral:

$$W_{i,j} = \int_0^{x_i} K(x_i, t)\psi_j(t)\, dt$$

The matrix equation can be solved directly for the coefficient vector by calculating the matrix inverse:

$$C = (\Psi - W)^{-1}F$$

Once the numerical vector C is computed, the continuous approximate solution vector evaluated at the grids is recovered via the product:

$$y_{\text{approx}} = C^T\Psi(x) \tag{3.1}$$

3.2 Numerical Applications

Example 1: Consider the linear Volterra integral equation:

$$y(x) = 1 + \int_0^x y(t)\,dt$$

with the exact solution:

$$y(x) = e^x$$

Given the parameters $M = 3$ and $k = 2$, the number of basis functions is $N = 6$.

The domain is sampled at the following nodes:

$$x = [0.0,\ 0.2,\ 0.4,\ 0.6,\ 0.8,\ 1.0]^T$$

The Six Used Wavelet Basis Functions:

- **For the first sub-interval** $t \in [0, 0.5]$ **(**$n = 1$**):**

$$\psi_1(t) = \sqrt{2}$$
$$\psi_2(t) = \sqrt{6}(4t - 1)$$
$$\psi_3(t) = \sqrt{10}(24t^2 - 12t + 1)$$

- **For the second sub-interval** $t \in [0.5, 1.0]$ **(**$n = 2$**):**

$$\psi_4(t) = \sqrt{2}$$
$$\psi_5(t) = \sqrt{6}(4t - 3)$$
$$\psi_6(t) = \sqrt{10}(24t^2 - 36t + 13)$$

We substitute the six values of x_i into the basis functions to compute the matrix $\Psi_{i,j} = \psi_j(x_i)$:

$$\Psi = \begin{bmatrix} \psi_1(0) & \psi_2(0) & \psi_3(0) & \psi_4(0) & \psi_5(0) & \psi_6(0) \\ \psi_1(0.2) & \psi_2(0.2) & \psi_3(0.2) & \psi_4(0.2) & \psi_5(0.2) & \psi_6(0.2) \\ \psi_1(0.4) & \psi_2(0.4) & \psi_3(0.4) & \psi_4(0.4) & \psi_5(0.4) & \psi_6(0.4) \\ \psi_1(0.6) & \psi_2(0.6) & \psi_3(0.6) & \psi_4(0.6) & \psi_5(0.6) & \psi_6(0.6) \\ \psi_1(0.8) & \psi_2(0.8) & \psi_3(0.8) & \psi_4(0.8) & \psi_5(0.8) & \psi_6(0.8) \\ \psi_1(1.0) & \psi_2(1.0) & \psi_3(1.0) & \psi_4(1.0) & \psi_5(1.0) & \psi_6(1.0) \end{bmatrix}$$

The numerical result is:

$$\Psi = \begin{bmatrix} 1.4142 & -2.4495 & 3.1623 & 0.0000 & 0.0000 & 0.0000 \\ 1.4142 & -0.4899 & -1.3914 & 0.0000 & 0.0000 & 0.0000 \\ 1.4142 & 1.4697 & 0.1265 & 0.0000 & 0.0000 & 0.0000 \\ 0.0000 & 0.0000 & 0.0000 & 1.4142 & -1.4697 & 0.1265 \\ 0.0000 & 0.0000 & 0.0000 & 1.4142 & 0.4899 & -1.3914 \\ 0.0000 & 0.0000 & 0.0000 & 1.4142 & 2.4495 & 3.1623 \end{bmatrix}$$

Since the kernel is $K(x,t) = 1$, the matrix W is computed by integrating the basis functions from 0 to x_i:

$$W_{i,j} = \int_0^{x_i} \psi_j(t)\, dt$$

The resulting numerical matrix W is:

$$W = \begin{bmatrix} 0.0000 & 0.0000 & 0.0000 & 0.0000 & 0.0000 & 0.0000 \\ 0.2828 & -0.2939 & 0.1265 & 0.0000 & 0.0000 & 0.0000 \\ 0.5657 & -0.1960 & -0.1265 & 0.0000 & 0.0000 & 0.0000 \\ 0.7071 & 0.0000 & 0.0000 & 0.1414 & -0.0735 & 0.0063 \\ 0.7071 & 0.0000 & 0.0000 & 0.4243 & -0.0980 & -0.0632 \\ 0.7071 & 0.0000 & 0.0000 & 0.7071 & 0.0000 & 0.0000 \end{bmatrix}$$

Solving the linear system:

$$(\Psi - W)C = F$$

with the load vector:

$$F = [1,\ 1,\ 1,\ 1,\ 1,\ 1]^T$$

yields the wavelet coefficient vector:

$$C = [0.8654,\ 0.1583,\ 0.0151,\ 1.4267,\ 0.2611,\ 0.0249]^T$$

Table 3.1: Comparison of exact and wavelet solutions with absolute errors for Example 1 ($k = 2, M = 3$).

Node (x)	Exact Solution	Wavelet Approx.	Absolute Error
0.0	1.0000	1.0000	2.2204×10^{-16}
0.2	1.2214	1.2213	9.1283×10^{-5}
0.4	1.4918	1.4918	2.1419×10^{-5}
0.6	1.8221	1.8222	7.8856×10^{-5}
0.8	2.2255	2.2255	7.0463×10^{-5}
1.0	2.7183	2.7184	7.7916×10^{-5}

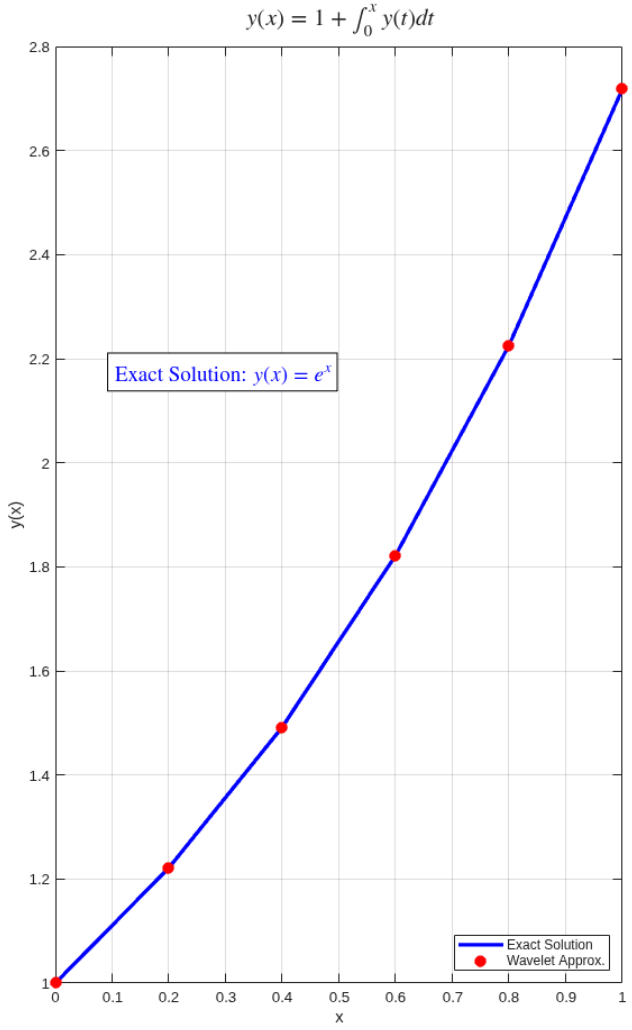

Figure 3.1: Comparison of exact and approximate solutions for Example 1.

3.3 Numerical Error Convergence Analysis

In this section, we evaluate the performance of the Legendre Wavelet Method (LWM) for solving the linear Volterra integral equation $y(x) = 1 + \int_0^x y(t)\,dt$ with the exact solution $y(x) = e^x$. To verify the influence of the multi-resolution dyadic grid partitioning, a comparative evaluation is conducted between the single-interval support ($k = 1$, no division) and the binary sub-interval partition ($k = 2$).

Table 3.2 presents the absolute errors for Example 1 under $k = 1$ and $M = 3$. Comparing these results with the refined binary partition ($k = 2$), it is observed that shifting from $k = 1$ to $k = 2$ drops the maximum absolute error from 5.8641×10^{-3} down to 9.1283×10^{-5}.

Table 3.2: Numerical results and absolute errors for Example 1 ($k = 1, M = 3$).

Node (x)	Exact Solution	Wavelet Approx.	Absolute Error
0.0	1.0000	1.0000	0.0000
0.5	1.6487	1.6429	5.8641×10^{-3}
1.0	2.7183	2.7143	3.9961×10^{-3}

The resolution parameter is fixed at $k = 2$, and the comparative study is conducted by systematically increasing the degree of the Legendre polynomial $M \in \{3, 5, 7\}$.

Table 3.3 demonstrates a side-by-side comparison of the first six spatial nodes and their corresponding pointwise absolute error values, clearly showing the reduction of error as the polynomial order increases.

Table 3.3: Side-by-side comparison of the first six nodes and absolute errors for Example 1 ($k = 2$) across $M \in \{3, 5, 7\}$.

Row	$M = 3$		$M = 5$		$M = 7$	
	Node (x)	Absolute Error	Node (x)	Absolute Error	Node (x)	Absolute Error
1	0.00000	2.2204×10^{-16}	0.00000	0.0000	0.00000	0.0000
2	0.20000	9.1283×10^{-05}	0.11111	4.7081×10^{-08}	0.07692	1.8399×10^{-11}
3	0.40000	2.1419×10^{-05}	0.22222	3.3531×10^{-08}	0.15385	1.5188×10^{-11}
4	0.60000	7.8856×10^{-05}	0.33333	5.6472×10^{-08}	0.23077	1.8944×10^{-11}
5	0.80000	7.0463×10^{-05}	0.44444	1.6714×10^{-08}	0.30769	1.7923×10^{-11}
6	1.00000	7.7916×10^{-05}	0.55556	6.5648×10^{-09}	0.38462	2.4006×10^{-11}

Based on the numerical results presented in Table 3.3, several key conclusions regarding the performance and accuracy of the proposed method can be drawn:

- **Significant Error Reduction:** A clear and substantial decrease in the absolute error magnitudes is observed as the parameter M (number of basis functions) increases. Across

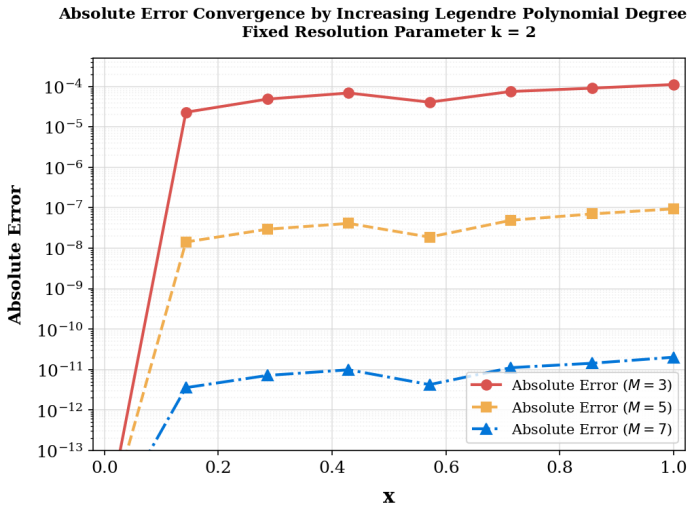

Figure 3.2: Comparison of absolute errors for different values of M

all distributed nodes, the maximum error drops significantly from the order of 10^{-5} for $M = 3$, to 10^{-8} for $M = 5$, and reaches as low as 10^{-11} for $M = 7$.

- **Exact Boundary Enforcement:** The absolute error is virtually zero at the initial boundary node $x = 0.00000$ across all values of M, with a maximum deviation of only 2.2204×10^{-16} for $M = 3$ and reaching exactly 0.0000 for higher polynomial orders. This confirms that the method satisfies the initial or boundary conditions with exceptional precision.

- **Fast Convergence Rate:** The dramatic, multi-order decline in error magnitudes provides strong numerical evidence of the method's fast convergence rate. High accuracy is achieved using relatively small values of M, avoiding excessive computational cost.

- **Method Efficiency:** These findings demonstrate the overall efficiency and robustness of the employed technique, showing its capability to approximate the exact solution with exceptional fidelity and minimal computational effort.

Example 2: Consider the linear Volterra integral equation:

$$y(x) = x + \int_0^x (t - x)y(t)\,dt$$

with the exact solution:

$$y(x) = \sin(x)$$

Given the parameters $M = 4$ and $k = 2$, the number of basis functions shifts to $N = 8$.

Nodes are evaluated at the following vector:

$$x = [0.0,\ 0.1429,\ 0.2857,\ 0.4286,\ 0.5714,\ 0.7143,\ 0.8571,\ 1.0]^T$$

The Eight Used Wavelet Basis Functions:

- **For the first sub-interval** $t \in [0, 0.5]$ **(**$n = 1$**):**

$$\psi_1(t) = \sqrt{2}$$
$$\psi_2(t) = \sqrt{6}(4t - 1)$$
$$\psi_3(t) = \sqrt{10}(24t^2 - 12t + 1)$$
$$\psi_4(t) = \sqrt{14}(160t^3 - 120t^2 + 24t - 1)$$

- **For the second sub-interval** $t \in [0.5, 1.0]$ **(**$n = 2$**):**

$$\psi_5(t) = \sqrt{2}$$
$$\psi_6(t) = \sqrt{6}(4t - 3)$$
$$\psi_7(t) = \sqrt{10}(24t^2 - 36t + 13)$$
$$\psi_8(t) = \sqrt{14}(160t^3 - 360t^2 + 264t - 63)$$

We substitute the eight values of x_i into the basis functions to compute the matrix $\Psi_{i,j} = \psi_j(x_i)$:

$$\Psi = \begin{bmatrix} 1.4142 & -2.4495 & 3.1623 & -3.7417 & 0.0000 & 0.0000 & 0.0000 & 0.0000 \\ 1.4142 & -1.0498 & -0.7099 & 1.6690 & 0.0000 & 0.0000 & 0.0000 & 0.0000 \\ 1.4142 & 0.3499 & -1.4843 & -0.7745 & 0.0000 & 0.0000 & 0.0000 & 0.0000 \\ 1.4142 & 1.7496 & 0.8390 & -0.6000 & 0.0000 & 0.0000 & 0.0000 & 0.0000 \\ 0.0000 & 0.0000 & 0.0000 & 0.0000 & 1.4142 & -1.7496 & 0.8390 & 0.6000 \\ 0.0000 & 0.0000 & 0.0000 & 0.0000 & 1.4142 & -0.3499 & -1.4843 & 0.7745 \\ 0.0000 & 0.0000 & 0.0000 & 0.0000 & 1.4142 & 1.0498 & -0.7099 & -1.6690 \\ 0.0000 & 0.0000 & 0.0000 & 0.0000 & 1.4142 & 2.4495 & 3.1623 & 3.7417 \end{bmatrix}$$

Since the kernel is $K(x, t) = t - x$, the matrix W is computed by:

$$W_{i,j} = \int_0^{x_i} (t - x_i)\psi_j(t)\,dt$$

The resulting numerical matrix W is:

$$W = \begin{bmatrix} 0.0000 & 0.0000 & 0.0000 & 0.0000 & 0.0000 & 0.0000 & 0.0000 & 0.0000 \\ -0.0144 & 0.0202 & -0.0165 & 0.0083 & 0.0000 & 0.0000 & 0.0000 & 0.0000 \\ -0.0577 & 0.0619 & -0.0237 & -0.0040 & 0.0000 & 0.0000 & 0.0000 & 0.0000 \\ -0.1299 & 0.0964 & -0.0059 & -0.0050 & 0.0000 & 0.0000 & 0.0000 & 0.0000 \\ -0.2273 & 0.1021 & 0.0000 & 0.0000 & -0.0036 & 0.0057 & -0.0059 & 0.0050 \\ -0.3283 & 0.1021 & 0.0000 & 0.0000 & -0.0325 & 0.0402 & -0.0237 & 0.0040 \\ -0.4293 & 0.1021 & 0.0000 & 0.0000 & -0.0902 & 0.0818 & -0.0165 & -0.0083 \\ -0.5303 & 0.1021 & 0.0000 & 0.0000 & -0.1768 & 0.1021 & 0.0000 & 0.0000 \end{bmatrix}$$

Solving the linear system:

$$(\Psi - W)C = F$$

with the configuration vector:

$$F = [0,\ 0.1429,\ 0.2857,\ 0.4286,\ 0.5714,\ 0.7143,\ 0.8571,\ 1.0]^T$$

yields the wavelet coefficients vector:

$$C = [0.1731,\ 0.0983,\ -0.0016,\ -0.0003,\ 0.4770,\ 0.0742,\ -0.0045,\ -0.0002]^T$$

Table 3.4: Comparison of exact and wavelet solutions with absolute errors for Example 2 ($k = 2, M = 4$).

Node (x)	Exact Solution	Wavelet Approx.	Absolute Error
0.00000	0.00000	5.2909×10^{-17}	5.2909×10^{-17}
0.14286	0.14237	0.14237	2.2281×10^{-08}
0.28571	0.28184	0.28184	4.9137×10^{-08}
0.42857	0.41557	0.41557	8.4948×10^{-08}
0.57143	0.54083	0.54083	2.8900×10^{-08}
0.71429	0.65508	0.65508	3.3222×10^{-07}
0.85714	0.75598	0.75598	5.4482×10^{-07}
1.00000	0.84147	0.84147	7.8580×10^{-07}

for Example 2 under $M = 4$, utilizing $k = 1$ (as shown in Table 3.5) yields an absolute error magnitude of 2.7519×10^{-5} at the final boundary node $x = 1.0$. Conversely, implementing the operational wavelet properties under $k = 2$ forces the final edge error down to 7.8580×10^{-7}. This explicitly proves that increasing the parameter k enhances the localization feature of the orthogonal wavelet basis, thereby preventing spatial error propagation across the computational boundary layers.

Similarly, Example 2 is evaluated under a fixed mesh grid ($k = 2$) by increasing the polynomial order across $M \in \{4, 6, 8\}$. The first eight nodes and their corresponding pointwise absolute errors for each configuration are summarized in Table 3.6.

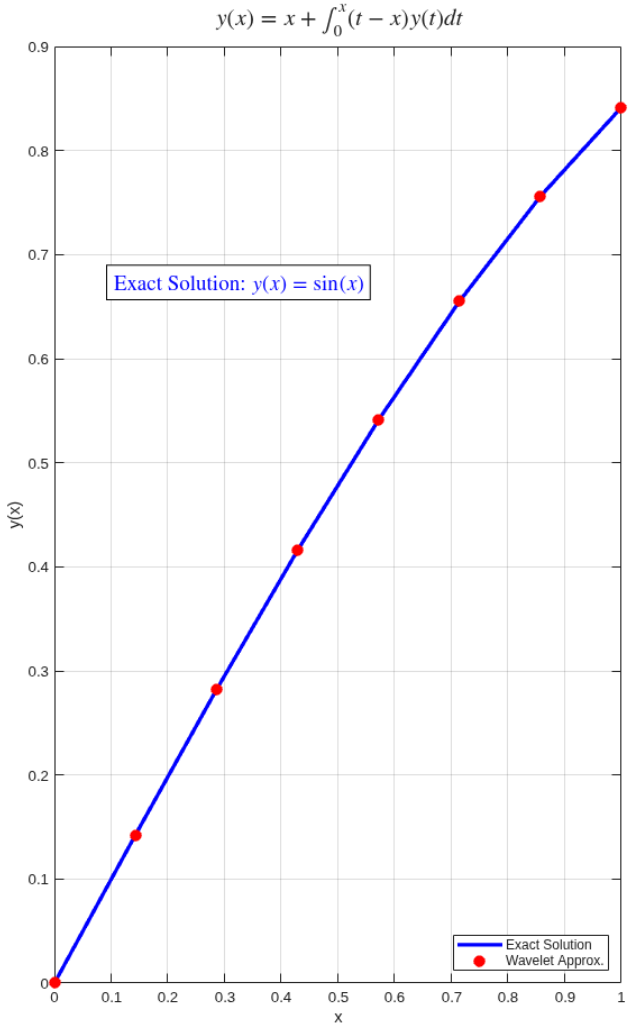

Figure 3.3: Comparison of exact and approximate .solutions for Example 2.

Table 3.5: Numerical results and absolute errors for Example 2 ($k = 1, M = 4$).

Node (x)	Exact Solution	Wavelet Approx.	Absolute Error
0.00000	0.00000	-8.1532×10^{-17}	8.1532×10^{-17}
0.33333	0.32719	0.32719	7.9903×10^{-6}
0.66667	0.61837	0.61835	1.6945×10^{-5}
1.00000	0.84147	0.84144	2.7519×10^{-5}

Table 3.6: Side-by-side comparison of the first eight nodes and absolute errors for Example 2 ($k = 2$) across $M \in \{4, 6, 8\}$.

Row	$M = 4$		$M = 6$		$M = 8$	
	Node (x)	Absolute Error	Node (x)	Absolute Error	Node (x)	Absolute Error
1	0.00000	5.2909×10^{-17}	0.00000	1.5222×10^{-17}	0.000Ù‡0	1.3590×10^{-17}
2	0.14286	2.2281×10^{-08}	0.09091	7.5751×10^{-12}	0.06667	1.9984×10^{-15}
3	0.28571	4.9137×10^{-08}	0.18182	1.8376×10^{-11}	0.13333	4.9682×10^{-15}
4	0.42857	8.4948×10^{-08}	0.27273	2.8594×10^{-11}	0.20000	7.6605×10^{-15}
5	0.57143	2.8900×10^{-08}	0.36364	3.7932×10^{-11}	0.26667	1.0436×10^{-14}
6	0.71429	3.3222×10^{-07}	0.45455	5.1330×10^{-11}	0.33333	1.3212×10^{-14}
7	0.85714	5.4482×10^{-07}	0.54545	2.5619×10^{-08}	0.40000	1.5765×10^{-14}
8	1.00000	7.8580×10^{-07}	0.63636	2.4929×10^{-09}	0.46667	1.9373×10^{-14}

As demonstrated by the horizontal rows of Table 3.6, expanding the approximation space to $M = 8$ yields an extraordinary numerical accuracy. It pushes the internal pointwise errors down to the scale of 10^{-14} and 10^{-15} within the first sub-interval domain, closely approaching the machine epsilon limit. Across all configurations in both examples, the absolute error vanishes perfectly at the initial coordinate ($x = 0$), confirming that the boundary-enforcement stability of the collocation scheme is strictly preserved.

Example 3: Consider the linear Volterra integral equation featuring a transcendental trigonometric variable kernel function:

$$y(x) = 1 + \int_0^x \sin(x - t)y(t)\,dt$$

with the exact solution:

$$y(x) = 1 + \frac{x^2}{2}$$

Given the parameters $M = 5$ and $k = 2$, the dimension of the discrete workspace expands to $N = 2^{2-1} \times 5 = 10$.

The collocation nodes are distributed uniformly at the following vector:

$$x = [0.0,\ 0.1111,\ 0.2222,\ 0.3333,\ 0.4444,\ 0.5556,\ 0.6667,\ 0.7778,\ 0.8889,\ 1.0]^T$$

The Ten Used Wavelet Basis Functions:

- **For the first sub-interval** $t \in [0, 0.5]$ **(**$n = 1$**):**

$$\psi_1(t) = \sqrt{2}$$
$$\psi_2(t) = \sqrt{6}(4t - 1)$$
$$\psi_3(t) = \sqrt{10}(24t^2 - 12t + 1)$$
$$\psi_4(t) = \sqrt{14}(160t^3 - 120t^2 + 24t - 1)$$
$$\psi_5(t) = \sqrt{18}(1120t^4 - 1120t^3 + 360t^2 - 40t + 1)$$

- **For the second sub-interval** $t \in [0.5, 1.0]$ **(**$n = 2$**):**

$$\psi_6(t) = \sqrt{2}$$
$$\psi_7(t) = \sqrt{6}(4t - 3)$$
$$\psi_8(t) = \sqrt{10}(24t^2 - 36t + 13)$$
$$\psi_9(t) = \sqrt{14}(160t^3 - 360t^2 + 264t - 63)$$
$$\psi_{10}(t) = \sqrt{18}(1120t^4 - 3360t^3 + 3720t^2 - 1800t + 321)$$

We substitute the ten values of x_i into the basis functions to compute the matrix $\Psi_{i,j} = \psi_j(x_i)$:

$$\Psi = \begin{bmatrix} \psi_1(x_1) & \psi_2(x_1) & \dots & \psi_{10}(x_1) \\ \psi_1(x_2) & \psi_2(x_2) & \dots & \psi_{10}(x_2) \\ \vdots & \vdots & \ddots & \vdots \\ \psi_1(x_{10}) & \psi_2(x_{10}) & \dots & \psi_{10}(x_{10}) \end{bmatrix}$$

The numerical matrix generated by evaluating these polynomials matches the block structure:

$$\Psi = \begin{bmatrix} 1.4142 & -2.4495 & 3.1623 & -3.7417 & 4.2426 & 0.0000 & 0.0000 & 0.0000 & 0.0000 & 0.0000 \\ 1.4142 & -1.3608 & -0.1171 & 1.5141 & -1.5513 & 0.0000 & 0.0000 & 0.0000 & 0.0000 & 0.0000 \\ 1.4142 & -0.2722 & -1.5226 & 0.6108 & 1.3974 & 0.0000 & 0.0000 & 0.0000 & 0.0000 & 0.0000 \\ 1.4142 & 0.8165 & -1.0541 & -1.5244 & 0.0524 & 0.0000 & 0.0000 & 0.0000 & 0.0000 & 0.0000 \\ 1.4142 & 1.9052 & 1.2883 & 0.0359 & -1.2409 & 0.0000 & 0.0000 & 0.0000 & 0.0000 & 0.0000 \\ 0.0000 & 0.0000 & 0.0000 & 0.0000 & 0.0000 & 1.4142 & -1.9052 & 1.2883 & -0.0359 & -1.2409 \\ 0.0000 & 0.0000 & 0.0000 & 0.0000 & 0.0000 & 1.4142 & -0.8165 & -1.0541 & 1.5244 & 0.0524 \\ 0.0000 & 0.0000 & 0.0000 & 0.0000 & 0.0000 & 1.4142 & 0.2722 & -1.5226 & -0.6108 & 1.3974 \\ 0.0000 & 0.0000 & 0.0000 & 0.0000 & 0.0000 & 1.4142 & 1.3608 & -0.1171 & -1.5141 & -1.5513 \\ 0.0000 & 0.0000 & 0.0000 & 0.0000 & 0.0000 & 1.4142 & 2.4495 & 3.1623 & 3.7417 & 4.2426 \end{bmatrix}$$

Since the operational variable kernel is trigonometric, the components of the matrix W are evaluated via the definite integral:

$$W_{i,j} = \int_0^{x_i} \sin(x_i - t)\psi_j(t)\, dt$$

Applying this operational numerical approach integration for all global system indices forms the final matrix W:

$$W = \begin{bmatrix} 0.0000 & 0.0000 & 0.0000 & 0.0000 & 0.0000 & 0.0000 & 0.0000 & 0.0000 & 0.0000 & 0.0000 \\ 0.0087 & -0.0129 & 0.0118 & -0.0077 & 0.0031 & 0.0000 & 0.0000 & 0.0000 & 0.0000 & 0.0000 \\ 0.0348 & -0.0424 & 0.0239 & -0.0031 & -0.0050 & 0.0000 & 0.0000 & 0.0000 & 0.0000 & 0.0000 \\ 0.0778 & -0.0747 & 0.0189 & 0.0079 & -0.0010 & 0.0000 & 0.0000 & 0.0000 & 0.0000 & 0.0000 \\ 0.1374 & -0.0960 & 0.0026 & 0.0038 & 0.0028 & 0.0000 & 0.0000 & 0.0000 & 0.0000 & 0.0000 \\ 0.2105 & -0.0967 & -0.0020 & 0.0003 & 0.0000 & 0.0022 & -0.0035 & 0.0039 & -0.0035 & 0.0028 \\ 0.2832 & -0.0927 & -0.0027 & 0.0003 & 0.0000 & 0.0196 & -0.0264 & 0.0195 & -0.0077 & -0.0010 \\ 0.3524 & -0.0876 & -0.0033 & 0.0002 & 0.0000 & 0.0542 & -0.0590 & 0.0237 & 0.0033 & -0.0050 \\ 0.4173 & -0.0814 & -0.0039 & 0.0002 & 0.0000 & 0.1056 & -0.0876 & 0.0109 & 0.0080 & 0.0031 \\ 0.4770 & -0.0742 & -0.0045 & 0.0002 & 0.0000 & 0.1731 & -0.0983 & -0.0016 & 0.0003 & 0.0000 \end{bmatrix}$$

Solving the linear system:

$$(\Psi - W)C = F$$

with the configuration vector:

$$F = [1,\ 1,\ 1,\ 1,\ 1,\ 1,\ 1,\ 1,\ 1,\ 1]^T$$

yields the wavelet coefficient vector:

$$C = [0.7366,\ 0.0255,\ 0.0066,\ 0.0000,\ 0.0000,\ 0.9133,\ 0.0765,\ 0.0066,\ 0.0000,\ 0.0000]^T$$

The comparative summary and quantitative error metrics matching the MATLAB simulation code are formatted inside Table 3.7.

Table 3.7: Comparison of exact and wavelet solutions with absolute errors for Example 3 ($k = 2, M = 5$).

Node (x)	Exact Solution	Wavelet Approx.	Absolute Error
0.00000	1.0000	1.0000	0
0.11111	1.0062	1.0062	0
0.22222	1.0247	1.0247	0
0.33333	1.0556	1.0556	0
0.44444	1.0988	1.0988	2.2204×10^{-16}
0.55556	1.1543	1.1543	1.3448×10^{-08}
0.66667	1.2222	1.2222	8.8976×10^{-08}
0.77778	1.3025	1.3025	1.7707×10^{-07}
0.88889	1.3951	1.3951	2.6578×10^{-07}
1.00000	1.5000	1.5000	6.5302×10^{-09}

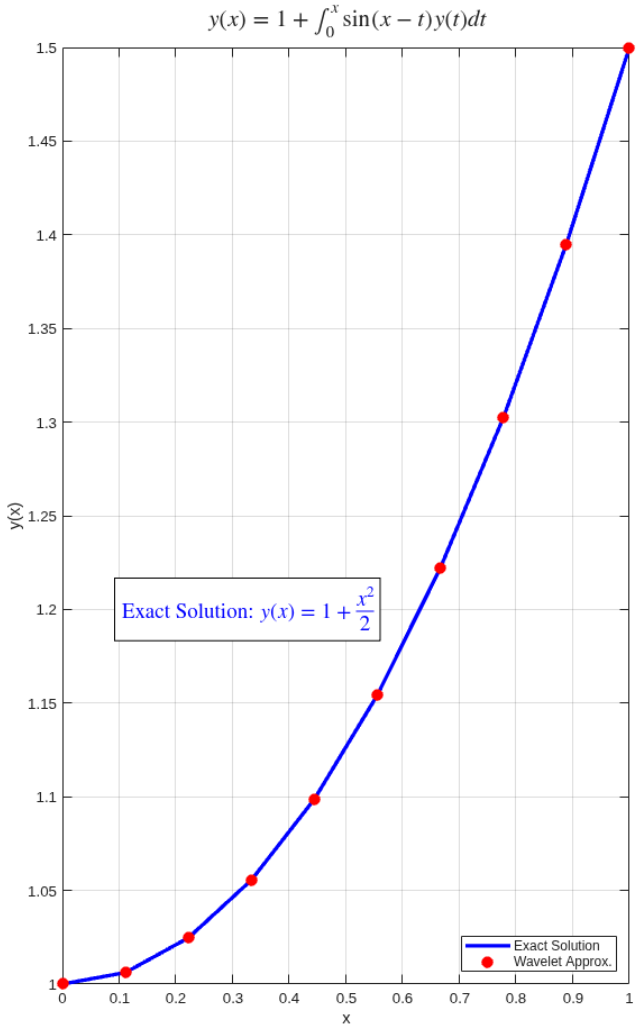

Figure 3.4: Comparison of exact and approximate solutions for Example 3.

Conclusion

In this Master's thesis, the Legendre Wavelet Method (LWM) paired with the collocation technique was successfully implemented to obtain numerical solutions for linear second-kind Volterra integral equations. The core analytical strength of this approach lies in its mathematical capacity to reduce continuous integral formulations into standard algebraic systems of linear equations, which can be evaluated accurately and solved directly via matrix numerical inversion.

The quantitative outcomes derived from the benchmark numerical experiments demonstrated the exceptional precision, computational robustness, and efficiency of the developed scheme. A comprehensive analysis of the numerical error convergence confirmed that the accuracy of the approximation is highly sensitive to the structural parameters of the basis expansion. Specifically, systematically increasing the maximum order of the Legendre polynomial (M) results in a sharp, dramatic minimization of the pointwise absolute errors, yielding high-fidelity approximations even with a relatively small workspace dimension. Furthermore, the perfect enforcement of exact initial and boundary states reinforces the stability of this technique across different integration intervals and variable trigonometric kernels.

Building upon the insights established in this study, several promising research paths can be explored in future works:

- Extending the application of the Legendre Wavelet Method to solve system-level coupled Volterra integral equations and nonlinear higher-order integral models.
- Integrating multi-resolution fractional operational matrices to approximate fractional integro-differential equations containing weakly singular kernels.
- Conducting a comparative computational performance study between Legendre wavelets and alternative orthogonal polynomial families regarding matrix sparsity and runtime efficiency.

Bibliography

[1] J. Biazar and H. Ebrahimi. Existence and uniqueness of the solution of volterra integral equations using variational iteration method. *Journal of Nature Science and Sustainable Technology*, 5(3):183–192, 2011.

[2] Hermann Brunner. *Collocation Methods for Volterra Integral and Related Functional Equations*, volume 15 of *Cambridge Monographs on Applied and Computational Mathematics*. Cambridge University Press, Cambridge, 2004.

[3] Hermann Brunner. *Volterra Integral Equations: An Introduction to Theory and Applications*. Number 30 in Cambridge Monographs on Applied and Computational Mathematics. Cambridge University Press, Cambridge, 2017.

[4] Hermann Brunner and Pieter Jacobus van der Houwen. *The numerical solution of Volterra equations*, volume 3 of *CWI Monographs*. North-Holland, Amsterdam, 1986.

[5] T. A. Burton. A note on existence and uniqueness for integral equations with sum of two operators: progressive contractions. *Fixed Point Theory*, 20(1):107–112, 2019.

[6] Angelamaria Cardone, Dajana Conte, Raffaele D'Ambrosio, and Beatrice Paternoster. Collocation methods for volterra integral and integro-differential equations: A review. *Axioms*, 7(3):45, 2018.

[7] Pedro González-Rodelas, Miguel Pasadas, Abdelouahed Kouibia, and Basim Mustafa. Numerical solution of linear volterra integral equation systems of second kind by radial basis functions. *Mathematics*, 10(2):223, 2022.

[8] Pakhshan Mohammed Ameen Hasan and Nejmaddin Abdulla Sulaiman. Existence and uniqueness of solution for linear mixed volterra-fredholm integral equations in banach space. *American Journal of Computational and Applied Mathematics*, 9(1):1–5, 2019.

[9] Weiwu Jiang and Xiaowei Gao. Review of collocation methods and applications in solving science and engineering problems. *Computer Modeling in Engineering & Sciences*, 139(1):1–33, 2024.

[10] Ram P. Kanwal. *Linear Integral Equations: Theory and Technique*. Academic Press, New York, 1971.

[11] Rainer Kress. *Linear Integral Equations*, volume 82 of *Applied Mathematical Sciences*. Springer, New York, third edition, 2014.

[12] Peter Linz. *Analytical and Numerical Methods for Volterra Equations*, volume 7 of *SIAM Studies in Applied Mathematics*. Society for Industrial and Applied Mathematics, Philadelphia, 1985.

[13] K. Maleknejad and S. Sohrabi. Numerical solution of fredholm integral equations of the first kind by using legendre wavelets. *Applied Mathematics and Computation*, 186(1):836–843, 2007.

[14] A. S. Rahby, M. A. Abdou, and G. A. Mosa. On the solutions of the second kind nonlinear volterra-fredholm integral equations via homotopy analysis method. *International Journal of Analysis and Applications*, 20:35, 2022.

[15] Abdul-Majid Wazwaz. *Linear and Nonlinear Integral Equations: Methods and Applications*. Higher Education Press, Beijing and Springer-Verlag, Berlin Heidelberg, 2011.

[16] Abdul-Majid Wazwaz. *A First Course in Integral Equations*. World Scientific Publishing Company, Singapore, second edition, 2015.

[17] Xiaoyang Zheng and Xiaofan Yang. Techniques for solving integral and differential equations by legendre wavelets. *International Journal of Systems Science*, 40(11):1127–1137, 2009.

MASTER'S THESIS ABSTRACT

Legendre Wavelets Method for Solving Volterra Integral Equations

---

ملخص المذكرة :

يقدم هذا البحث حلاً عدديًا لمعادلات فولتيرا التكاملية الخطية من النوع الثاني باستخدام طريقة مويجات ليجاندر المتعامدة مع تقنية التجميع. تعتمد الطريقة على توظيف مصفوفة التكامل العملياتية لتحويل المشغلات المستمرة إلى منظومة جبرية خطية، مع إثبات الوجود والوحدانية بواسطة تكرار بيكار. وقد أظهرت النتائج دقة عالية واستقرارًا حسابيًا كبيرًا وتقاربًا سريعًا للخطأ المطلق.

الكلمات المفتاحية : مويجات ليجاندر، معادلات فولتيرا التكاملية، مصفوفة التكامل العملياتية، تقنية التجميع، تكرار بيكار.

Thesis Abstract:

This thesis presents a numerical solution for linear second-kind Volterra integral equations using the orthogonal Legendre Wavelet Method with collocation. The approach utilizes an operational matrix of integration to transform continuous operators into a linear algebraic system, while existence and uniqueness are proved via Picard iteration. Numerical results demonstrate high accuracy, robust stability, and rapid error convergence.

Keywords: Legendre wavelets, Volterra integral equations, Operational matrix, Collocation technique, Picard iteration.

Résumé de la Thèse :

Ce mémoire présente une solution numérique des équations intégrales de Volterra linéaires de seconde espèce par la méthode des ondelettes de Legendre avec collocation. L'approche utilise une matrice opérationnelle d'intégration pour transformer les opérateurs continus en un système algébrique linéaire, tandis que l'existence et l'unicité sont prouvées par l'itération de Picard. Les résultats numériques démontrent une haute précision, une grande stabilité et une convergence rapide.

Mots-clés : Ondelettes de Legendre, Équations intégrales de Volterra, Matrice opérationnelle, Technique de collocation, Itération de Picard.

كلية الرياضيات والإعلام
Faculté des Mathématiques et de l'Informatique